Tropical Plant Biology (2025) 18:6
https://doi.org/10.1007/s12042-024-09375-z

RESEARCH

Mapping of Major QTLs Conferring Higher Branching Numbers in Backcross Introgression Lines of *Sinapis alba* + *Brassica juncea* Somatic Hybrids

Preetesh Kumari[1] · Kaushal Pratap Singh[2] · Pramod Kumar Rai[2]

Received: 25 July 2024 / Accepted: 7 September 2024
© The Author(s), under exclusive licence to Springer Science+Business Media, LLC, part of Springer Nature 2024

Abstract

Sinapis alba genome has been utilized as a donor for abiotic and biotic stress tolerance, yet there seems to be a gap in exploring its potential contribution to yield-related traits. The greater number of lateral branches in Brassica plants provides new sites for bearing siliquae and emphasizes their profound impact on yield potential. The present investigation involves the morphological characterization of 94 backcross introgression lines (BCILs) over two consecutive crop seasons, coupled with genotyping by 277 *S. alba* genome-specific monoallelic microsatellite markers to decipher the genetic loci contributing to higher branching number traits. The results revealed significant QTLs governing primary (PB) and secondary branching (SB). In CS-I, two QTLs linked to PB collectively explained 46.50% of the phenotypic variance (PVE), exhibiting positive additive effects, signifying their contribution to increased branch numbers in BCILs. Two QTLs associated with SB were also identified, with LODs of 5.07 and 4.21 contributing 22.55 and 17.90%, respectively, to the PVE. During the CS-II, one QTL was identified for PB, explaining 28.04% of the PVE at a 20.97 LOD value, and one major QTL for SB was identified (27.52% of the PVE). Moreover, we also identified 40 potential genes within the QTL regions, with sixteen genes homologous to the *ANT*, *MAX2*, *PNH*, *RAX2*, *SEU*, *CRE1*, and *RAMOSUS1 of Arabidopsis and pea*, and a total of nine unknown genes with a role in branching that were introgressed from *S. alba* to *B. juncea*. This is the first study to identify introgressed candidate genes involved in *Brassica* branching.

Keywords BCILs · Primary and secondary branching · RAX2 and SEU gene introgressions · *Sinapis alba* · *Sinapis*-specific SSRs · Stable QTLs

Introduction

Brassica juncea (L.) Czern & Coss (2*n* = 36, AABB), a vital oilseed crop known for its edible oil, holds global prominence in cultivation. Over the period from 2010 to 11 to 2018-19, a remarkable increase in productivity and production occurred, with values increasing from 1840 kg/ha to 1980 kg/ha and from 61.64 million metric tons to 72.42 million metric tons, respectively (https://www.drmr.res.in/about_rmcrop.php). The linkage map of *B. juncea* demonstrates the conservation and unchanged nature of the parental genomes (*B. nigra* and *B. rapa*) since hybridization (Axelsson et al. 2000). The genetic homogeneity across cultivated varieties of *B. juncea* limits yield augmentation through hybridization between the species. However, hybridization results in heterosis and introduces transgressive phenotypes, including novel phenotypic variation not observed in the parents (Dittrich-Reed and Fitzpatrick 2013). Moreover, hybridization between closely related genera is an extensive and regular evolutionary process (Arnold and Meyer 2006; Mallet 2007; Soltis and Soltis 2009). However, hybridization among genera, particularly those with diverse base chromosome numbers, can also lead to improper chromosome pairing during meiosis and result in poor fertility (Bird et al. 2021). The appropriate bivalent formation of homologous chromosomes in such intergeneric hybrids can be restored

Communicated by: Marcelo Dornelas

✉ Kaushal Pratap Singh
kaushalmpi1978@gmail.com

[1] Genetics Division, ICAR-Indian Agricultural Research Institute, Pusa campus, New Delhi 110012, India

[2] ICAR-Directorate of Rapeseed Mustard Research, Sewar, Bharatpur 321303, India

Published online: 23 October 2024

through somatic hybridization with good fertility and seed set (Kumari et al. 2020c).

A large number of wild members of the family Brassicaceae, including *B. tournifortii*, *Diplotaxis catholica*, *Moricandia arvensis*, *Sinapis arvensis*, *S. alba*, and *Trichystoma ballii*, have been utilized as donors for biotic and abiotic stress tolerance by developing somatic hybrids (Kirti et al. 1992a, b, 1995; Wang et al. 2005; Kumari et al. 2018, 2020c, 2022). We have developed and reported stable and fertile somatic hybrids of *B. juncea* and *S. al*ba to introgress resistance to major diseases, including Alternaria blight and Sclerotinia stem rot, along with high temperature and drought tolerance. The Backcross Introgression Lines (BCILs) were developed to improve resistance and yield contributing traits in the *B. juncea* (cultivated parent) genome background. However, the second BCILs showed superiority to many yield contributing traits over cultivated parent *B. juncea* such as basal branching, primary and secondary branching, siliquae length, seeds/siliqua, test weight, etc. (Kumari et al. 2018; Kumari and Bhat 2019, 2021; Kumari and Singh 2019; Singh et al. 2023). However, the wild species are known for inferior yield potential and quality traits. Cultivars with inferior yield potential and tolerance to stresses are not suitable for commercial cultivation. Therefore, it is necessary to work with dual objectives simultaneously, i.e., identifying the genes of the donor parent that are responsible for the yield penalty as well as identifying the genes that contribute to the high yield potential (Kumari et al. 2024a, b). Plant architecture, such as branching number, is directly associated with yield performance in the case of *B. juncea*. Bushy branching patterns significantly enhance the potential yield by creating additional sites for flowers and subsequent seed development, concurrently optimizing light interception to facilitate efficient photosynthesis (Reinhardt and Kuhlemeier 2002; Sarlikioti et al. 2011).

Remarkably, *S. alba* stands distinguished by its heightened number of primary and secondary branches, surpassing *B. juncea* and other allied members within the Brassicaceae family (Kumari et al. 2011; Singh et al. 2023). The regulation of shoot branching and its intricate patterns encompasses various developmental stages, including node patterning, the emergence of axillary meristems within leaf axils, and the subsequent growth of axillary buds (Hempel and Feldman 1994; Shimizu-Sato and Mori 2001; Grbic and Bleecker 2000; Ward and Leyser 2004; McSteen and Leyser 2005). The determination of branch numbers is a multifactorial process subject to the influence of climatic conditions (Grbic and Bleecker 2000; Rameau et al. 2015; Aguilar et al. 2007; Cline 1996; Ongaro and Leyser 2008; Ferguson and Beveridge 2009). Branch elongation is regulated by a consortium of phytohormones, including auxin, cytokinin, and abscisic acid (Shimizu-Sato et al. 2009; Ward and Leyser, 2004). Branch development is regulated by the hormones *AUXIN RESISTANT1* (*AXR1*) (Lincoln et al. 1990; Leyser et al. 1993; Stirnberg et al. 1999) and *MORE AXILLARY GROWTH* (*MAX*) (Stirnberg et al. 2002; Sorefan et al. 2003; Booker et al. 2005; Bennett et al. 2006) through the regulation of auxin signaling and transport. This intricate network is fortified by additional genes governing node patterning in *A. thaliana*, including *REVOLUTA* (*REV*) (Talbert et al. 1995), *SHOOT MERISTEMLESS* (*STM*) (Long et al. 1996), *LATERAL SUPPRESSOR* (*LAS*) (Greb et al. 2003), and the *REGULATORS OF AXILLARY MERISTEMS* (*RAX*) genes (Keller et al. 2006; Muller et al. 2006). The inflorescence meristem identity is defined by floral identity genes, including *TERMINAL FLOWER1* (*TFL1*) (Bradley et al. 1997) and *LEAFY* (*LFY*) (Weigel et al. 1992). Numerous genes encoding key components, such as arabinogalactan proteins, cytochrome P450 enzymes, MAPKK7, and various DNA-binding proteins, have been identified for their significant roles in orchestrating the process of branch outgrowth (Nambeesan et al. 2015).

Out of total 24 S. alba chromosomes, the presence of 6 chromosomes along with segmental introgressions in B. juncea chromosomes, it is not feasible to go for transcriptome or GBS to decipher the role of S. alba in the development of higher primary and secondary branch numbers in second BCILs. Due to the proximity of the *S. alba* and *B. juncea* genomes, appropriate pairing during meiosis has been observed between the chromosomes of somatic hybrids and their backcrossed progeny (Kumari et al. 2018, 2020b, c). Therefore, the scarcity of polymorphic molecular markers among parents is a problem because of the high degree of homology among chromosomes (Nelson and Lydiate, 2006). After the search for the genome of *S. alba* that was dissimilar from that of Brassica oilseed progenitors, stepwise removal of the matched genome was performed, which yielded only 17.06% unmatched genomes. The genetic closeness of approximately 83% of similar genomic regions to cultivated Brassicas has also been demonstrated, as documented in earlier studies (Lysak et al. 2005; Singh et al. 2022b). To overcome this challenge and the scarcity of polymorphic simple sequence repeats (SSRs) in Brassica, a breakthrough emerged with the development of 1107 *S. alba* genome-specific monoallelic microsatellite markers from the unmatched genome (Kumari et al. 2020a; Singh et al. 2022b). These distinctive microsatellite markers, uniquely tailored to the *S. alba* genome, play a pivotal role in deciphering the genetic architecture of traits such as Alternaria blight resistance, plant height, and siliquae-related traits in backcross lines derived from the allohexaploid Brassicas (Singh et al. 2021b; Kumari et al. 2024a, b). Notably, the core set of BCILs employed in the present study exhibited remarkable stability and a high degree of gametic fertility. In this study, we (i) constructed a linkage map of BCILs, (ii) performed QTL analysis and (iii) identified candidate genes

for primary and secondary branches in the 94 backcrossed lines of S. alba and B juncea.

Results

Morphological Characterization of PB and SB

The number of primary and secondary branches exhibited substantial variability among the BCILs. During the CS-I, the PB ranged from a minimum of 2.0 to a maximum of 21.0, while the SB ranged from 0.0 to 57.0. In the subsequent CS-II, there was an increase in the numbers, with PB ranging from 3.0 to 27.0 and SB increasing to a range of 0.0 to 99.0 (Fig. 1A-D). The grand mean values for PB in CS-I and CS-II were 6.38 ± 0.77 and 7.78 ± 0.75, respectively. Similarly, the grand mean values for SB were 14.24 ± 3.06 and 18.44 ± 3.43 for the same CSs, respectively. These observations revealed significant variations in both PB and SB across two consecutive CSs.The highest average PB was consistently observed in the branching trait donor parent *S. alba* (18.00 and 23.40, respectively) while the B. juncea parent was recorded to 4.8 and 9.2, respectively during the two crop seasons. This was followed by notable averages for BCILs 3 (10.40), 43 (9.60), 16, and 82 (9.40) for CS-I and for BCILs 92 (11.40), 40 (11.20), 77 (10.60), and 13 (10.20) for CS-II. Similarly, the highest average SB was consistently found for the trait donor parent *S. alba* (43.60 and 81.80, respectively) whereas the B. juncea parent was recorded for 10.4 and 27.2 SB, respectively across the two crop seasons. This was followed by prominent averages in BCILs such as 10 (26.20), 83 (24.00), 77 (23.60), and 27 (22.80) for the CS-I and BCILs 9 (32.00), 92 (31.60), 75 (29.40), 74, and 77 (28.00) for the CS-II. Conversely, the minimum average PB was observed in BCILs 35, 66 (4.40), 60 (4.20), 56 (4.00), and 70 (2.60) for CS-I. In the subsequent CS-II, the minimum average PB was recorded in BCILs 28 (5.60), 68 (5.40), 72, 78 (5.20), and 46 (4.40). Likewise, the minimum average SB was recorded in BCILs 66, 70 (7.20), 28 (7.00), 32 (6.60), and 49 (5.00) for CS-I. In CS-II, this minimum average SB was documented in BCILs 20, 87 (8.80), 36 (8.60), 49 (8.40), and 84 (8.00).

The cumulative effects of environmental and genotypic variations play a pivotal role in determining the observed phenotypic variations. For the PB trait, the phenotypic coefficient of variation (PCV) was 37.22 for CS-I and 57.67 for CS-II. Likewise, for SB, the PCV values were 33.40 in CS-I and 59.10 in CS-II. Remarkably, the PCV values surpassed

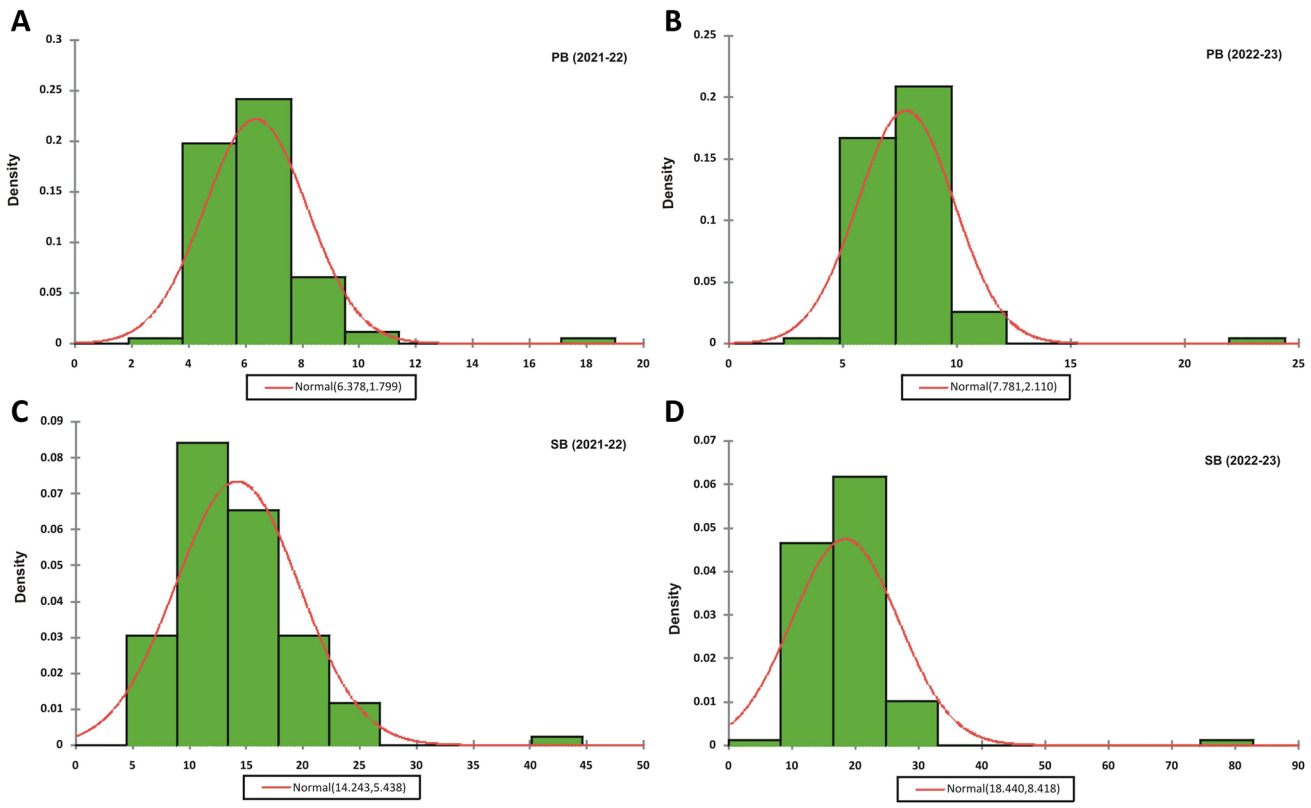

Fig. 1 The mean phenotypic distributions of PB (**A**, **B**) and SB (**C**, **D**) during the 2021-22 and 2022-23 crop seasons, respectively. The grand mean value and standard deviation (StDev) are presented at the bottom of the graph

the genotypic coefficient of variation (GCV) values for both traits, underscoring the substantial influence of environmental factors on branching traits. The PB and SB traits exhibited commendable broad-sense heritability (H2b) values, indicating that these traits were especially affected by genetic factors rather than being predominantly governed by environmental conditions. However, the genetic variability associated with these traits was comparatively low. The percentages of the mean genetic advancement (GAM) were 36.67 and 36.55 for PB and 40.06 and 61.32 for SB, respectively (Table 1). This study revealed a robust genotypic and phenotypic correlation between PB and SB in both crop seasons. This correlation was effectively visualized through a correlation heatmap (Fig. 2A, B). The analysis of the scree plot highlighted the predominant role of the first factor (F1), contributing to 73.98% of the total phenotypic variability. Similarly, F2, F3, and F4 contributed 14.52%, 8.41%, and 3.09%, respectively, to the variability. The cumulative contribution of these factors effectively encapsulated the entirety of the variability (Fig. 3A). Principal component analysis (PCA) elucidated the distribution of active variables (PB and SB) for CS-I and CS-II across the first and second quadrants, respectively. Interestingly, these first two principal components cumulatively accounted for 88.50% of the variability in both traits. Furthermore, a remarkably strong positive correlation between PB and SB traits was depicted in the correlation circle across both crop seasons (Fig. 3B).

Linkage Map

A set of 277 monoallelic *S. alba* genome-specific microsatellite markers ranging in product size from 100 to 400 base pairs, derived from a draft genome assembly, was used for genotyping the core group of 94 BCILs alongside their parents (*S. alba* and *B. juncea*) (Singh et al. 2022b). The specificity of these markers for the donor genome was verified by their successful amplification in *S. alba* but failure to amplify in *B. juncea*, and these markers effectively behaved as dominant markers rather than exhibiting a natural codominant nature. The linkage groups were constructed through QTLIciMapping software, and a total of 12 linkage groups (LGs) were constructed similar to the haploid chromosome numbers of the trait donor parent. The constructed linkage groups collectively spanned a length of 1866.17 centiMorgan (cM). Among these, LG-10 had the shortest length, measuring 62.66 cM, while LG-04 exhibited the longest length, at 293.70 cM. Furthermore, the analysis revealed that the maximum marker interval was observed on LG-09, spanning a distance of 56.55 cM, while the minimum marker distance was recorded on LG-11, with an interval of 0.27 cM. LG-04 displayed the greatest number of markers, totaling 35, while the lowest marker count (13) was detected for LG-10 (Fig. 4).

QTL Mapping

The morphological data of the BCILs from the BC_2F_{6-7} generations, focusing on PB and SB, were precisely recorded over two consecutive crop seasons (CS-I and CS-II) at the ICAR-DRMR. The recorded genotyping data of the BCILs, in combination with their morphological traits, were employed to conduct QTL mapping utilizing the ICIM-ADD function with dominance effects. During the CS-I, a total of 4 distinct QTLs were successfully mapped within the BCIL

Table 1 The statistical findings of PB and SB were evaluated in a core set of 94 backcross lines (BCILs) along with *S. Alba* and *B. Juncea* parents during the 2021-22 and 2022-23 crop seasons

S. No.	Particulars	Primary Branches*		Secondary Branches*	
		2021-22	2022-23	2021-22	2022-23
1	Maximum	21.0000	27.0000	57.0000	99.0000
2	Minimum	2.0000	3.0000	0.0000	0.0000
3	Grand Mean	6.3771	7.7812	14.2438	18.4396
4	Standard Error of Mean (SEm)	0.7666	0.7513	3.0567	3.4336
5	Critical Difference (CD) 5%	2.1317	2.0892	8.4998	9.5477
6	Critical Difference (CD) 1%	2.8068	2.7508	11.1912	12.5710
7	Environmental Variance	2.9386	2.8226	46.7186	58.9485
8	Genotypic Variance	2.6938	3.9332	20.7626	59.8159
9	Phenotypic Variance	5.6324	6.7558	67.4812	118.7644
10	Environmental Coefficient of Variance	26.8813	21.5910	47.9866	41.6376
11	Genotypic Coefficient of Variance	25.7372	25.4873	31.9902	41.9428
12	Phenotypic Coefficient of Variance	37.2156	33.4033	57.6723	59.1006
13	Heritability (Broad Sense)	0.4783	0.5822	0.3077	0.5037
14	Genetic Advance	2.3382	3.1173	5.2066	11.3068
15	Genetic Advance as percentage of mean	36.6657	40.0617	36.5536	61.3181

*Significant at $P = 0.001$

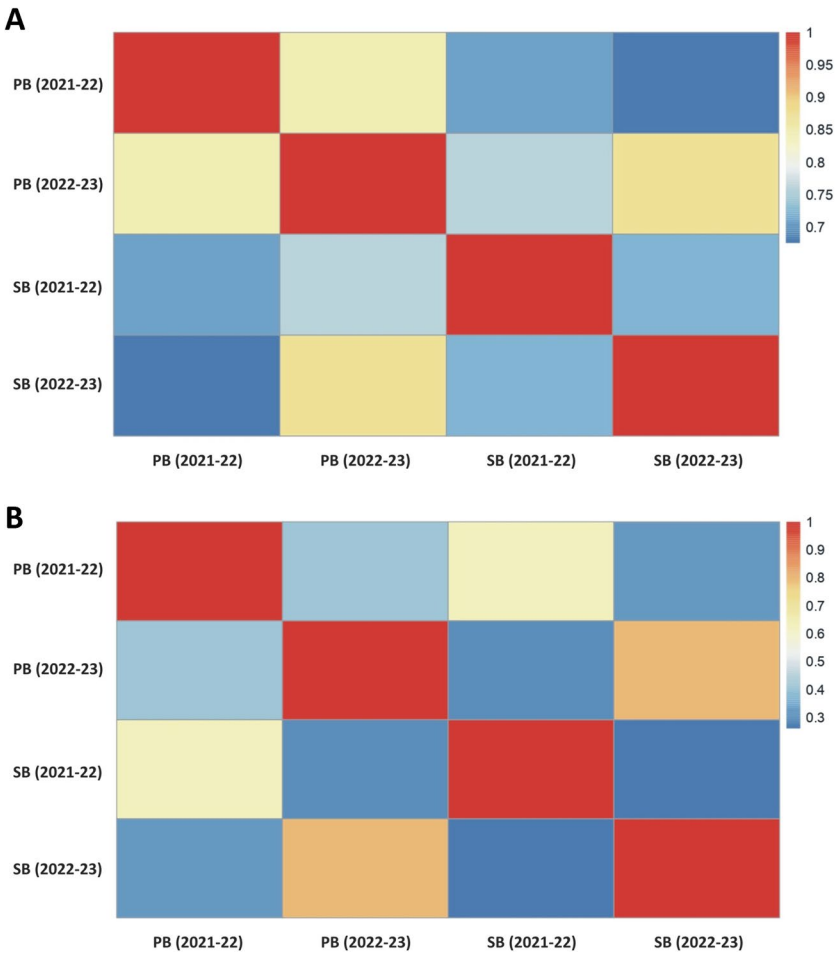

Fig. 2 Genetic (**A**) and phenotypic (**B**) correlations between PB and SB during the 2021-22 and 2022-23 crop seasons

genome for both the PB and SB traits. Among these identified QTLs, two were specifically associated with PB (marked by **red** squares in Fig. 4), while the other two QTLs contributed to SB (denoted by a **green** circle in Fig. 4). The two PB-associated QTLs were localized within LG-01 and LG-12 at 106.00 and 62.00 cM, respectively, each accompanied by LODs of 6.56 and 6.06, respectively. Remarkably, these QTLs contributed to 24.90% and 21.66% of the phenotypic variation, respectively. Conspicuously, these two QTLs were considered major due to their substantial influence, accounting for more than 10% of the phenotypic variation in the PB trait. The microsatellite markers Sa78003 and Sa56608 were identified as the closest markers for these two PB QTLs. Overall, these two major PB QTLs collectively explained more than 46% of the phenotypic variation. For the SB trait, two major QTLs were identified within LG-01 and LG-02 (at positions of 106.00 and 18.00 cM, respectively), among which the first QTL was found to be closely linked with the PB QTL. These SB QTLs had LOD scores of 5.07 and 4.21 and contributed to 22.55 and 17.90% of the phenotypic variation, respectively. The nearest microsatellite markers associated with these SB QTLs were Sa78003 and Sa267264 (Fig. 5A). During CS-I, the identified QTLs displayed positive additive effects, with values of 2.92, 2.12, 6.43, and 3.99, respectively. These additive effects highlighted the estimated impact of the QTL at the current scanning position. In contrast, the dominance effects (indicating the estimated dominance effect of the QTL at the current scanning position) for these QTLs exhibited negative and positive values of -1.63, 0.75, 0.63, and − 2.87, respectively (Table 2).

In the subsequent CS-II, the QTL analysis yielded the identification of a total of three QTLs associated with PB and SB, positioned on LG-01 and LG-08. Within this set, one QTL was associated with PB, while two QTLs were associated with the SB trait. This PB-associated QTL (represented by a **blue** triangle in Fig. 4) exhibited an LOD of 20.97 within LG-01 at 107.00 cM. This QTL explained a total of 28.04% of the phenotypic variation and is considered a major QTL for PB. Additionally, one major QTL was detected for the SB trait (indicated by **pink** stars in Fig. 4), located within LG-01 at an LOD value of 21.40. This SB QTL contributed 27.52% of the phenotypic variation, showing a positive additive effect (19.44) and a negative dominance effect (-21.30). Notably, both of these QTLs for PB and SB were major and situated at the same genetic position

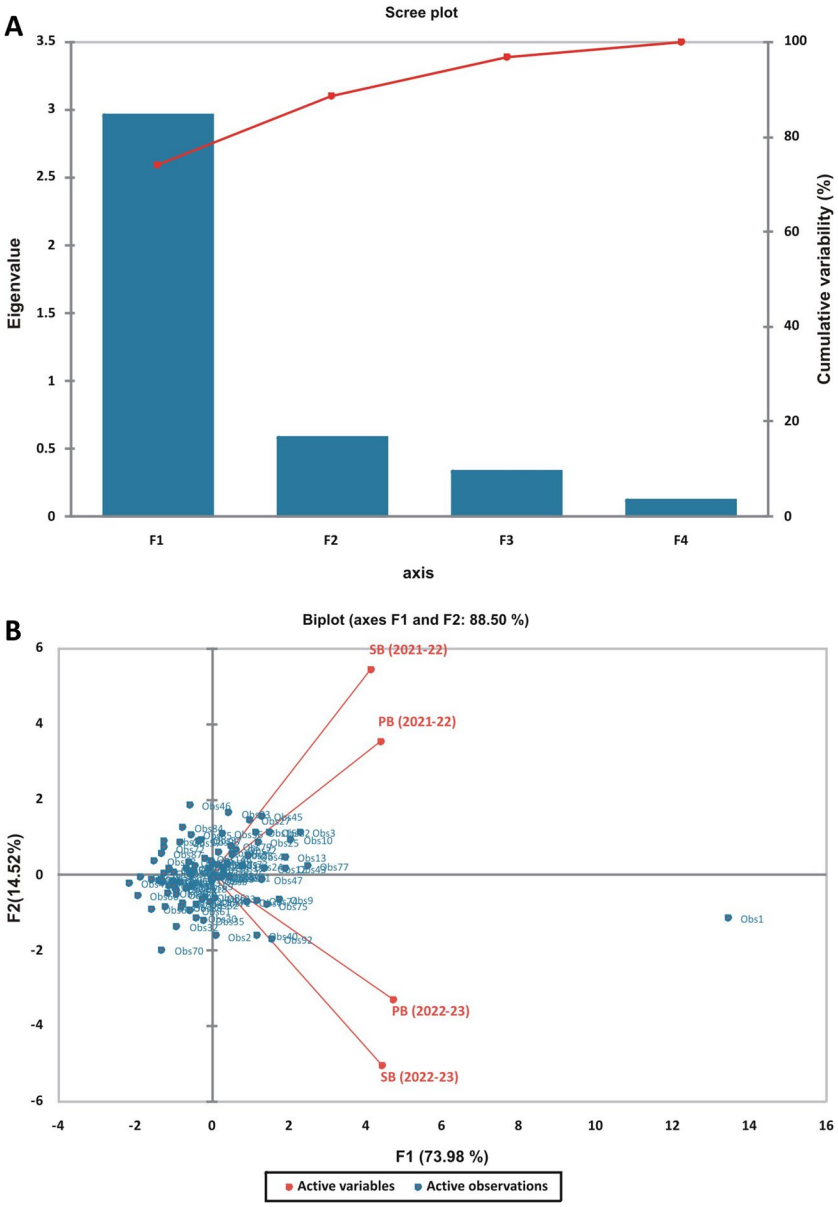

Fig. 3 **A** A scree plot showing the eigenvalues of the F1, F2, F3, and F4 factors and their percent cumulative effects on the phenotypes; **B** Principal component analysis (PCA) between observations (BCILs) and circles of correlation between variables (PB and SB for the 2021-22 and 2022-23 crop seasons) (numbers on the axes represent the correlation coefficients)

(107.00 cM) within LG-01, specifically between the microsatellite markers Sa78003 and Sa215207. This proximity suggested a tight linkage between PB and SB QTLs and showed positive (4.70 and 19.44) and negative (-7.12 and −21.30) additive and dominance effects, respectively. Moreover, the remaining QTL of SB was identified within LG-08 neighboring the microsatellite marker Sa39267 at 3.00 cM at a LOD value of 2.77, explaining only 2.22% of the phenotypic variation (Fig. 5B; Table 2). Thus, this minor QTL can be considered insignificant and was ignored in this study.

Gene Prediction and Candidate Gene Identification

The AUGUSTUS web server yielded a total of 40 predicted genes (PGs) from the QTL regions of PB and SB. To confirm their possible presence in the genome of BCILs, these PGs were BLAST with the H1 allohexaploid transcriptome assembly, which is one of the parents of the BCILs. The BLAST analysis confirmed the presence of all 40 PGs in the BGC genome. (Table S1). Further analysis involved BLASTN comparisons of these 40 PGs with a set of 1127 branching genes (BGs) downloaded from the ENA database. The results indicated that a total of twenty-five PGs matched with BGs, showing sequence identities ranging from 83.33 to 100%. PG-1, PG-7, PG-8, PG-13, PG-14, PG-23, PG-24, PG-25, and PG-29 were annotated as uncharacterized genes of *A. thaliana*, while PG-9, PG-15, PG-16, PG-17, PG-19, PG-20, PG-22, PG-27, PG-28, PG-32, PG-34, PG-35, PG-36, PG-37, PG-38, and PG-40 were annotated as *ANT*, *LEAFY*, *MAX2*, *PNH*, *RAX2*, *SEU*, *CRE1*, auxin resistance

protein 3, *embryonic flower 1*, and *RAMOSUS1* genes of *A. thaliana* and pea (Table S2). Moreover, the PGs were subjected to BLASTN comparisons with the nucleotide collection (nr) database of NCBI through the CLC Genomics Workbench. Out of the total PGs, a total of 36 PGs were found to be hit with the sequences of the database selected *A. thaliana* as the reference plant (Table S3). Further BLAST annotations were conducted with reference RNA sequences (refseq-rna), resulting in successful annotation for all PGs, with similarities ranging from 96 to 100% (Table S4). Annotations were also carried out using the expressed sequence tag (est) database of NCBI, which successfully annotated 39 PGs with similarities ranging from 86 to 100% (Table S5). Similarly, the genomic survey sequence (gss) database of NCBI was used for annotation, yielding sequence similarities between 79% and 100% (Table S6). Among the PGs, only 10 exhibited a sequence identity below 100% with the patented sequence (pat), while the others were successfully annotated with absolute similarity (Table S7). Protein translation of the PGs, except for PG-6, was subjected to BLASTP comparisons with the nonredundant protein sequences (nr) showing a sequence identity between 31 and 100%. The PG-24 and PG-25 were found to match absolutely to a protein-coding gene for pyrophosphorylase 2, which is essential for both vegetative and reproductive phases in Arabidopsis (Table S8). PG-24 and PG-25 were again annotated for the pyrophosphorylase 2 gene of *A. thaliana* in the reference proteins (refseq_protein) database, while few PGs were repeatedly annotated for polyketide synthase, aldehyde dehydrogenase 6B2, tubby-like protein 2, and the ankyrin repeat family protein of *A. thaliana* (Table S9). Among the total PGs, 39 PGs were successfully found to match sequences in the UniProtKB/Swiss-Prot protein sequence (Swiss-Prot) database with varying levels of similarity (31–95%). The PGs were again annotated for functions similar to those in other protein and nucleotide sequence databases (Table S10).

Discussion

S. alba is frequently used as a trait donor for introducing resistance against numerous abiotic and biotic stresses in cultivated germplasms of rapeseed and mustard (Hansen and Earle, 1997; Li et al. 2009, Kumari et al. 2018, 2023; Wang et al. 2014). We identified *S. alba* as having a bushy plant architecture and having high numbers of primary and secondary branches compared to those of other members of the tribe Brassiceae (Kumari et al. 2011). The additional branches result in the generation of a new site for flower, siliquae, and seed development, which substantially influences yield enhancement (Ehrenreich et al. 2007; Yaish et al. 2010; Singh et al. 2023). However, alien gene introgressions into crop species have several difficulties, such as pre- and post fertilization incompatibility, inadequate chromosomal pairings and resultant hybrid sterility, and the persistence of unfavorable linked traits or linkage drags (Kirti et al. 1992b; Agrawal et al. 2021, Bohra et al. 2022). We have efficiently exploited the feasibility of gene introgression for several abiotic and abiotic tolerance, including tolerance to Alternaria blight, Sclerotinia stem rot, and high temperature and drought stresses, from *S. alba* to *B. juncea* (Kumari et al. 2018; Kumari and Singh 2019; Kumari et al. 2020b, 2023; Singh et al. 2021b, 2022b, 2023). We are fortunate to find aggregate chromosomal pairings not only in somatic hybrids of *S. alba* and *B. juncea* but also in their first and second backcrossed progeny, which results in high fertility (Kumari et al. 2020b, c; Singh et al. 2023). However, the impact of linkage drag toward plant height, main shoot length, siliquae length, and number of seeds/siliquae has been observed in some BCILs (Kumari et al. 2024a, b). In this study, we identified candidate genes that contribute to greater numbers of primary and secondary branches via a set of 277 monoallelic SSR markers derived from only 17.06% of unmatched sequences in the *S. alba* genome (Singh et al. 2022b). They were uniquely designed to amplify only in the donor genome (*S. alba*) and failed to amplify in the genome of other crop Brassicas, including *B. rapa*, *B. nigra*, *B. oleracea*, *B. carinata*, *B. juncea*, and *B. napus*. Moreover, we also eliminated the matched sequences of the organelle genomes (chloroplasts and mitochondria) of the cultivated Brassica plants. Thus, these SSR markers efficiently identified the alleles introgressed uniquely into a set of 94 BCILs from the *S. alba* genome.

The identification of genetic loci associated with branch numbers is essential for unraveling the hereditary mechanisms governing branching morphogenesis. This insight has valuable implications for the significant improvement of the plant architecture of the crop Brassica through breeding strategies. Earlier studies have demonstrated the effect of environmental factors, including planting density and nutrient availability, on branching patterns (Casal et al. 1986; Aguilar et al. 2007; Napoli and Ruehle, 1996; Cline, 1991). BCILs represent an advanced generation and are characterized by substantial allelic diversity. This variation is created by the introgression of nearly half of the haploid genome of *S. alba*, either as segmental or additional chromosomal introgressions (Kumari et al. 2018, 2020b, c; Kumari and Bhat 2019, 2021). Due to this extensive allelic variation within the core set of BCILs, conducting association analysis via SNP genotyping became unfeasible. Consequently, in this study, an alternative reverse genetics approach was adopted to elucidate the genes responsible for the higher numbers of PBs and SB in a select group of 94 *S. alba-B. juncea* BCILs (Singh et al. 2023).

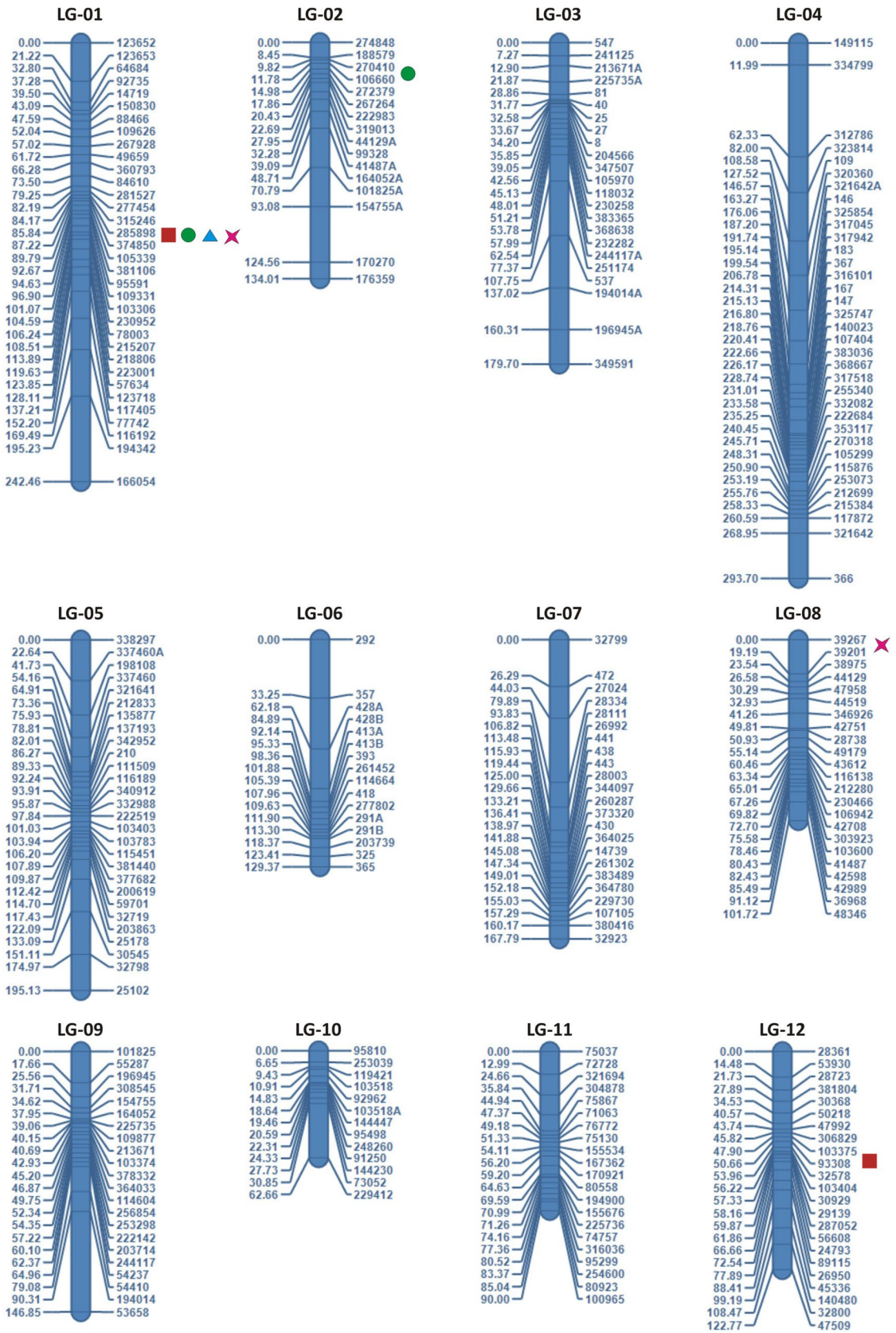
LG-01
0.00 123652
21.22 123653
32.80 64684
37.28 92735
39.50 14719
43.09 150830
47.59 88466
52.04 109626
57.02 267928
61.72 49659
66.28 360793
73.50 84610
79.25 281527
82.19 277454
84.17 315246
85.84 285898
87.22 374850
89.79 105339
92.67 381106
94.63 95591
96.90 109331
101.07 103306
104.59 230952
106.24 78003
108.51 215207
113.89 218806
119.63 223001
123.85 57634
128.11 123718
137.21 117405
152.20 77742
169.49 116192
195.23 194342
242.46 166054
LG-02
0.00 274848
8.45 188579
9.82 270410
11.78 106660
14.98 272379
17.86 267264
20.43 222983
22.69 319013
27.95 44129A
32.28 99328
39.09 41487A
48.71 164052A
70.79 101825A
93.08 154755A
124.56 170270
134.01 176359
LG-03
0.00 547
7.27 241125
12.90 213671A
21.87 225735A
28.86 81
31.77 40
32.58 25
33.67 27
34.20 8
35.85 204566
39.05 347507
42.56 105970
45.13 118032
48.01 230258
51.21 383365
53.78 368638
57.99 232282
62.54 244117A
77.37 251174
107.75 537
137.02 194014A
160.31 196945A
179.70 349591
LG-04
0.00 149115
11.99 334799
62.33 312786
82.00 323814
108.58 109
127.52 320360
146.57 321642A
163.27 146
176.06 325854
187.20 317045
191.74 317942
195.14 183
199.54 367
206.78 316101
214.31 167
215.13 147
216.80 325747
218.76 140023
220.41 107404
222.66 383036
226.17 368667
228.74 317518
231.01 255340
233.58 332082
235.25 222684
240.45 353117
245.71 270318
248.31 105299
250.90 115876
253.19 253073
255.76 212699
258.33 215384
260.59 117872
268.95 321642
293.70 366
LG-05
0.00 338297
22.64 337460A
41.73 198108
54.16 337460
64.91 321641
73.36 212833
75.93 135877
78.81 137193
82.01 342952
86.27 210
89.33 111509
92.24 116189
93.91 340912
95.87 332988
97.84 222519
101.03 103403
103.94 103783
106.20 115451
107.89 381440
109.87 377682
112.42 200619
114.70 59701
117.43 32719
122.09 203863
133.09 25178
151.11 30545
174.97 32798
195.13 25102
LG-06
0.00 292
33.25 357
62.18 428A
84.89 428B
92.14 413A
95.33 413B
98.36 393
101.88 261452
105.39 114664
107.96 418
109.63 277802
111.90 291A
113.30 291B
118.37 203739
123.41 325
129.37 365
LG-07
0.00 32799
26.29 472
44.03 27024
79.89 28334
93.83 28111
106.82 26992
113.48 441
115.93 438
119.44 443
125.00 28003
129.66 344097
133.21 260287
136.41 373320
138.97 430
141.88 364025
145.08 14739
147.34 261302
149.01 383489
152.18 364780
155.03 229730
157.29 107105
160.17 380416
167.79 32923
LG-08
0.00 39267
19.19 39201
23.54 38975
26.58 44129
30.29 47958
32.93 44519
41.26 346926
49.81 42751
50.93 28738
55.14 49179
60.46 43612
63.34 116138
65.01 212280
67.26 230466
69.82 106942
72.70 42708
75.58 303923
78.46 103600
80.43 41487
82.43 42598
85.49 42989
91.12 36968
101.72 48346
LG-09
0.00 101825
17.66 55287
25.56 196945
31.71 308545
34.62 154755
37.95 164052
39.06 225735
40.15 109877
40.69 213671
42.93 103374
45.20 378332
46.87 364033
49.75 114604
52.34 256854
54.35 253298
57.22 222142
60.10 203714
62.37 244117
64.96 54237
79.08 54410
90.31 194014
146.85 53658
LG-10
0.00 95810
6.65 253039
9.43 119421
10.91 103518
14.83 92962
18.64 103518A
19.46 144447
20.59 95498
22.31 248260
24.33 91250
27.73 144230
30.85 73052
62.66 229412
LG-11
0.00 75037
12.99 72728
24.66 321694
35.84 304878
44.94 75867
47.37 71063
49.18 76772
51.33 75130
54.11 155534
56.20 167362
59.20 170921
64.63 80558
69.59 194900
70.99 155676
71.26 225736
74.16 74757
77.36 316036
80.52 95299
83.37 254600
85.04 80923
90.00 100965
LG-12
0.00 28361
14.48 53930
21.73 28723
27.89 381804
34.53 30368
40.57 50218
43.74 47992
45.82 306829
47.90 103375
50.66 93308
53.96 32578
56.22 103404
57.33 30929
58.16 29139
59.87 287052
61.86 56608
66.66 24793
72.54 89115
77.89 26950
88.41 45336
99.19 140480
108.47 32800
122.77 47509

◂**Fig. 4** The linkage map of 94 BCILs (BC_2F_{6-7}) developed by QTLIciMapping using 277 *S. alba* genome-specific microsatellite markers revealed 12 linkage groups (LG-1 to LG-12). The red squares and green circles indicate QTLs for PB and SB in CS-I, while the blue triangles and pink stars denote QTLs for PB and SB identified in CS-II. The marker position and SSR number are shown on the left and right sides of the linkage groups, respectively

Ungerer et al. (2002, 2003) conducted QTL mapping studies in A. thaliana and identified 10 loci that may be responsible for branching variation. In the present study, we identified 7 loci that regulate PB and SB in BCILs during two consecutive crop seasons. Among the total PB QTLs over two seasons, three major QTLs were identified as being independently responsible for 24.90, 21.66, and 28.04% of the phenotypic variation. Among these three major QTLs, the first two QTLs were identified during CS-I, and the remaining QTLs were identified during CS-II. The cumulative effect of environment, genotype, and interactions between them regulate branching morphogenesis in brassicas. Nonetheless, there were only two (LOD: 5.07, 4.21) and one (LOD: 21.40) major QTL identified during the two crop seasons for SB. Moreover, the identification of major QTLs for PB and SB within LG-1 repeatedly during both crop seasons at approximately the same position confirmed their stability. All the QTLs for PB and SB detected during the crop seasons exhibited positive additive effects, except for a minor QTL for SB in CS-II, which exhibited a negative additive effect. This minor QTL explained only 2.22% of the phenotypic variation; thus, this QTL was not considered significant and was not used for candidate gene identification. The positive and negative effects explain the role of loci in increasing (by additive gene action) and decreasing a particular trait, respectively (Kumari et al. 2024a). We detected strong genotypic and phenotypic correlations between PB and SB during both crop seasons as clear from Fig. 2. Therefore, the correlation studies of both traits throughout both crop seasons confirmed the proximity of the PB and SB QTLs. Genetic mechanisms that influence phenotypic variation can operate not only at the level of gene structure but also by affecting gene expression. The six significant QTLs for PB and SB yielded a total of 40 genes that were annotated by BLAST for putative functions. Among the total genes predicted from these QTL regions, nine PGs were homologous to uncharacterized genes of *A. thaliana*, while 16 PGs were annotated as *ANT*, *LEAFY*, *MAX2*, *PNH*, *RAX2*, *SEU*, *CRE1*, auxin resistance protein 3, *Embryonic Flower 1*, and *RAMOSUS1* genes of *A. thaliana* and pea, respectively (Ehrenreich et al. 2007).

ANT promotes the initiation of floral organ primordia at specific positions within the floral meristem and prevents the premature differentiation of both primordial and floral meristem cells (Krizek et al. 2020). A candidate gene homologous to *ANT* was identified in the present study within LG-1 associated with the PB and SB traits. In *Arabidopsis*, the *LEAFY* (*LFY*; At5g61850) gene participates in floral meristem configuration and regulates floral meristem identity by establishing the expression of the MADS-box floral homeotic genes responsible for floral organ identity (Chahtane et al. 2018). PG-15, identified within LG-12 for the PB QTL close to the Sa56608 microsatellite, showed absolute BLAST similarity with the *LFY* gene. The *PINHEAD* (*PNH*; At5g43810) gene identified within the QTL region of PB (PG-17) has a role in the formation of the normal primary shoot apical meristem in angiospermic plants during embryogenesis and lateral shoot apical meristems arising postembryonically in the axils of leaves (Ehrenreich et al. 2007; Zhu et al. 2011). The *PNH* mutants exhibited defects in axillary meristem development, which is the mechanism by which plants develop new indeterminate growth axes after embryogenesis (McConnell and Barton 1995; Moussian et al. 2006; Lynn et al. 1999). Analyses of genes that appear to regulate auxin transport, such as the *MORE AXILLARY GROWTH-2* (*MAX-2*) gene identified in LG-12 at the PB QTL region, have revealed the central role of this hormone in coordinating branch outgrowth with the plant developmental program (Stirnberget al. 2002; Sorefan et al. 2003; Booker et al. 2005; Bennett et al. 2006). Four copies of the *REGULATOR OF AXILLARY MERISTEMS-2* (*RAX2*; At2g36890) gene (homologous to PG-19, -20, -22, and −35) were identified in the QTL regions of PB and SB located within LG-12 and LG-2. The *RAX2* genes identified in the QTL regions encode the R2R3 MYB transcription factors that have been shown to regulate the development of axillary meristems in Arabidopsis (Jia et al. 2020).

The three copies of the *SEUSS* (*SEU*; At1g43850) gene identified in the QTL region were homologous to those of PG-27, PG-32, and PG-38. This gene forms a physical complex with the LEUNIG transcriptional coregulator in Arabidopsis. (Bao et al. 2010; Gong et al. 2016; Huai et al. 2018). PG-28 is homologous to the *cytokinin response 1* (*CRE1*; At2g01830) gene, which plays a central role in root growth, leaf development, shoot initiation, formation and maintenance of meristem activity, senescence, and reproductive growth (Haberer and Kieber 2001; Higuchi et al. 2004; Nishimura et al. 2004). The *CRE1* mutant was identified in a screen for mutants impaired in the cell division, greening, and shoot formation responses of callus tissue to cytokinin (Inoue et al. 2001). Biochemical, molecular, and genetic studies have suggested that auxin resistance protein 3 (AXR3; At1g04250; homologous to PG-34) plays a central role in auxin signaling and plant development (Ouellet et al. 2001). The two copies of *the embryonic flower 1* (*EMF1*; At5g11530) gene were found to be homologous to those of PG-36 and PG-37 and to function as a transcription repressor that regulates phase transition during shoot,

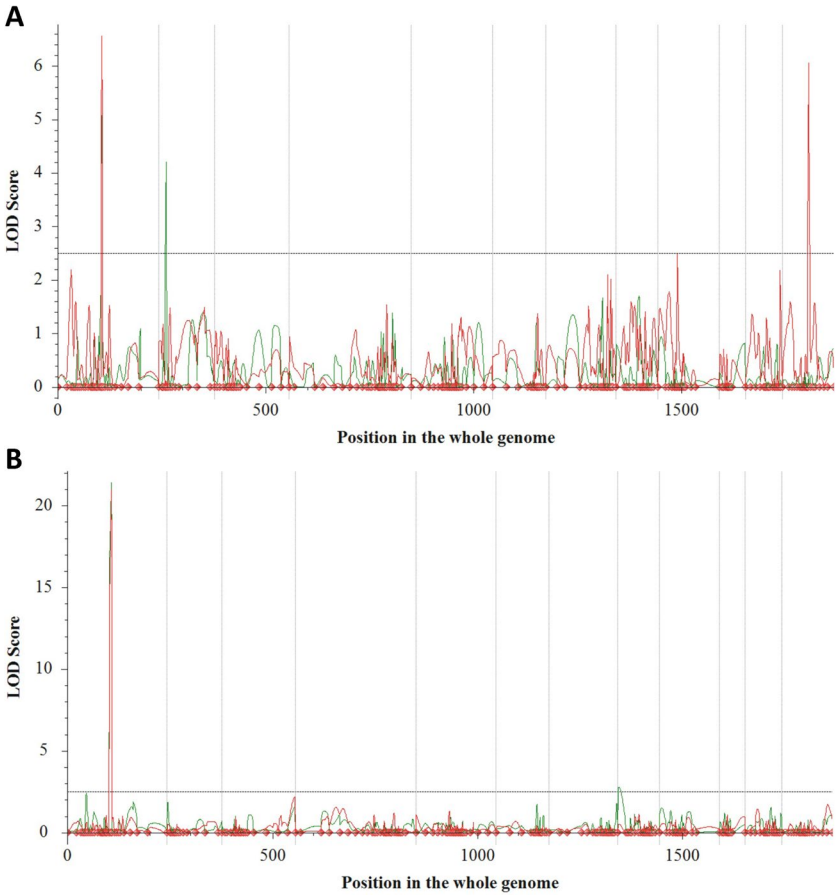

Fig. 5 The positions of the QTLs for the PB (red) and SB (green) traits in the BCILs (BC_2F_{6-7}) of allohexaploid Brassica in the DRMR region of Bharatpur during the 2021-22 (**A**) and 2022-23 (**B**) crop seasons. The map size on the x-axis is indicated in centi-Morgan (cM), and the LG is separated by vertical lines. The horizontal dotted line shows the LOD threshold for QTL identification

Table 2 The QTLs detected for PB and SB in a subpopulation of 94 BCILs (BC_2F_6) developed from the somatic hybrid of *B. juncea* + *S. Alba* at DRMR, Bharatpur (India) during the 2021-22 (CS-I) and 2022-23 (CS-II) crop season

S. No.	Trait name	CS	LG	Position (cM)	Left marker	Right marker	LOD	PVE (%)	Add	Dom	Cl (cM)
1	PB	I	1	106.00	230,952	**78,003**	6.55	24.89	2.92	-1.63	105.50 ~ 106.50
2	PB	I	12	62.00	**56,608**	24,793	6.05	21.66	2.12	0.75	61.50 ~ 63.50
3	SB	I	1	106.00	230,952	**78,003**	5.07	22.54	6.43	0.63	105.50 ~ 106.50
4	SB	I	2	18.00	**267,264**	222,983	4.20	17.89	3.99	-2.87	16.50 ~ 18.50
5	PB	II	1	107.00	**78,003**	215,207	20.96	28.03	4.69	-7.11	106.50-107.50
6	SB	II	1	107.00	**78,003**	215,207	21.40	27.52	19.44	-21.30	106.50-107.50
7	SB	II	8	3.00	**39,267**	39,201	2.76	2.21	-1.92	-2.02	0.00-13.50

*closest marker to QTL (shown by bold numbers)

CS Crop Season, *LOD* logarithm of the odds, *PVE* phenotypic variance, *Add* additive effect, *Dom* dominance effect, *CI* confidence interval

flower, and seed development. It controls leaf development, shoot architecture, and flowering by delaying both the vegetative to reproductive transition and flower initiation (Aubert et al. 2001). The *RAMOSUS1* (*RMS1*) gene of *Pisum sativum*, which is homologous to *MAX4* (At4g32810) from Arabidopsis, was found to be homologous to PG-40, which actively regulates shoot branching via physiologically defined mobile signals (Foo et al. 2005; Sorefan et al. 2003). The *S. alba*-specific SSR markers were found closest to the QTLs and could be used in marker-assisted selection (MAS) breeding because of the greater number of branches.

Materials and Methods

Plant Materials

The backcross introgression lines (BCILs) utilized in this study were derived from two stable somatic hybrids, known as H1 and H2. These hybrids were developed from successful somatic cell fusion between *S. alba* and *B. juncea*. The development of BCILs was achieved through backcrossing with *B. juncea* RLM-198, a methodology that we previously reported (Kumari et al. 2018, 2020b). To facilitate a comprehensive assessment of QTLs related to primary (PB) and secondary branching (SB), a core set of 94 BCILs from the BC_2F_{6-7} generation, along with their parents (*S. alba* and *B. juncea*), were characterized for phenotypic traits and simultaneously genotyped with SSRs for QTL mapping.

Experimental Design

The experimental field was prepared in mid-October, during the two subsequent crop seasons denoted as CS-I for the 2021-22 season and CS-II for the 2022-23 season. The BCILs were properly sown within the field, ensuring a precise separation of 45 cm between rows and 30 cm between individual plants. This strategic spacing allowed sufficient space to promote natural growth and development. To maintain uniform conditions, the cultivation of BCILs adhered to established agronomic practices. A standardized set of agricultural practices was upheld throughout the growth period, with the sowing schedule meticulously synchronized for both crop seasons, namely, CS-I and CS-II.

Morphological Characterization and Statistical analysis

Morphological variations in both PB and SB were carefully recorded upon the maturity of the BCIL plants. The field-based investigation was conducted at the ICAR-Directorate of Rapeseed Mustard Research in Bharatpur, India (coordinates: E 77°27'27", N 27°11'57", elevation: 178.37 msl). To record the data, the PB and SB traits of five arbitrarily selected plants from each BCIL were recorded. The dataset spanned both crop seasons, and the data collected independently for each season underwent subsequent statistical analysis and QTL mapping. The complete set of BCILs was sown in a randomized block design (RBD) with three replications of each line. Various parameters, including the standard error of the mean (SEm), critical difference at 5% and 1% (CD), broad-sense heritability (Hb2), analysis of variance (ANOVA), environmental variation (EV), genotypic variation (GV), phenotypic variation (PV), coefficient of variation (CV), and frequency distribution of the core set of 94 BCILs and their parents, were meticulously assessed by employing the variability package (https://CRAN.R-project.org/package=variability; Singh and Chaudhary 1977) within R v4.2.1. Additionally, utilizing the same package, the genotypic and phenotypic correlations between PB and SB for two years were analyzed. Statistical analysis of phenotypic data was performed for distribution fitting (histogram) development using agglomerative hierarchical clustering XLSTAT 2024 software (Addinsoft 2024).

DNA Extraction, Genotyping, and QTL Mapping

The genomic DNA of the BCILs in the BC_2F_{6-7} generation, along with that of their parents, was extracted from fresh young leaves using a modified CTAB method outlined by Kirti et al. (1995). The concentration of the extracted DNA was quantified using a Nanodrop-8000 spectrophotometer (Thermo Fisher Scientific, USA). A comprehensive set of 277 monoallelic SSR markers of the trait donor parent *S. alba* was used to genotype the 94 BCIL lines of the BC_2F_{6-7} generation (Kumari et al. 2020a; Singh et al. 2022b). The PCR conditions were the same as those reported previously (Kumari et al. 2024a). The genotyping data from the 94 BCILs, characterized using 277 microsatellite markers, were used for the construction of a genetic linkage map and QTL identification in association with phenotypic data. Genetic linkage map construction and QTL mapping for the BCILs were carried out by utilizing the QTLIciMapping software v4.1 (Meng et al. 2015). The detailed procedure for linkage mapping and QTL identification was described in a previous study (Singh et al. 2021a).

Candidate Gene Search

The QTLs identified for PB and SB across both crop seasons were subjected to gene prediction using the AUGUSTUS web server (https://bioinf.uni-greifswald.de/augustus/submission.php), with *A. thaliana* chosen as the reference organism. In this context, the major QTL regions associated with PB and SB were employed for predicting putative genes, except for a minor QTL. For the annotation of these predicted genes, a dataset containing 1127 genes (with a cumulative length of 58,40,929 bp) of PB and SB in FASTA format was obtained from the European Nucleotide Archive (ENA; https://www.ebi.ac.uk/ena/browser/home) on September 15, 2022. These predicted genes were then subjected to local BLASTN analysis against the aforementioned downloaded genes. This operation was performed using CLC Genomics Workbench version 20.0.4 (Qiagen, USA). Subsequently, to further confirm the possible presence of these predicted genes in the BCILs, the predicted genes were BLASTN compared with the recently developed

transcriptome assembly of the H1 allohexaploid (Singh et al. 2022a). For comprehensive annotation, these predicted genes were subjected to additional BLASTN/P analysis against various databases, including the nucleotide collection (nr), reference RNA sequence (refseq_rna), expressed sequence tag (est), genomic survey sequence (gss), patent sequence (pat), nonredundant protein sequence (nr), reference protein (refseq_protein), and UniProtKB/Swiss-Prot protein sequence (Swissprot) databases. This annotation process was executed using the CLC Genomics Workbench.

Supplementary Information The online version contains supplementary material available at https://doi.org/10.1007/s12042-024-09375-z.

Author Contributions PK: developed the somatic hybrids and their backcross progenies, conceived the study, and finalization of the manuscript; KPS: developed the BCILs, conducted field trials for both years, phenotyping, field data analysis, genotyping, QTL mapping, editing, and finalization of the manuscript; PKR: Provided laboratory and field facilities, monitor the study, read the manuscript. All the authors have read the final version of the manuscript and approved it for submission.

Funding None.

Data Availability No datasets were generated or analysed during the current study.

Declarations

Ethics Approval and Consent to Participate Not Applicable.

Consent for Publication Informed consent was obtained from all individual participants included in the study.

Competing Interests The authors declare no competing interests.

References

Addinsoft (2024) XLSTAT statistical and data analysis solution. New York, USA. https://www.xlstat.com/en

Agrawal N, Gupta M, Atri C, Akhatar J, Kumar S, Heslop-Harrison PJS, Banga SS (2021) Anchoring alien chromosome segment substitutions bearing gene(s) for resistance to mustard aphid in *Brassica juncea-B. fruticulosa* introgression lines and their possible disruption through gamma irradiation. Theor Appl Genet 134(10):3209–3224. https://doi.org/10.1007/s00122-021-03886-z

Aguilar-Martínez JA, Poza-Carrión C, Cubas P (2007) *Arabidopsis* BRANCHED1 acts as an integrator of branching signals within axillary buds. Plant Cell 19:458–472

Arnold ML, Meyer A (2006) Natural hybridization in primates: one evolutionary mechanism. Zoology 109:261–276

Aubert D, Chen L, Moon YH, Martin D, Castle LA, Yang CH, Sung ZR (2001) EMF1, a novel protein involved in the control of shoot architecture and flowering in Arabidopsis. Plant Cell 13(8):1865–1875. https://doi.org/10.1105/tpc.010094

Axelsson T, Bowman CM, Sharpe AG, Lydiate DJ, Lagercrantz U (2000) Amphidiploid *Brassica juncea* contains conserved progenitor genomes. Genome 43(4):679–688

Bao F, Azhakanandam S, Franks RG (2010) SEUSS and SEUSS-LIKE transcriptional adaptors regulate floral and embryonic development in *Arabidopsis*. Plant Physiol 152(2):821–836. https://doi.org/10.1104/pp.109.146183

Bennett T, Sieberer T, Willett B, Booker J, Luschnig C et al (2006) The Arabidopsis MAX pathway controls shoot branching by regulating auxin transport. Curr Biol 16:553–563

Bird KA, Niederhuth CE, Ou S, Gehan M, Pires JC, Xiong Z, Buren RV, Edger PP (2021) Replaying the evolutionary tape to investigate subgenome dominance in allopolyploid *Brassica napus*. New Phytol 230:354–371

Bohra A, Kilian B, Sivasankar S, Caccamo M, Mba C, McCouch SR, Varshney RK (2022) Reap the crop wild relatives for breeding future crops. Trends Biotechnol 40(4):412–431. https://doi.org/10.1016/j.tibtech.2021.08.009

Booker J, Sieberer T, Wright W, Williamson L, Willett B et al (2005) MAX1 encodes a cytochrome P450 family member that acts downstream of MAX3/4 to produce a carotenoid-derived branch-inhibiting hormone. Dev Cell 8:443–449

Bradley D, Ratcliffe O, Vincent C, Carpenter R, Coen E (1997) Inflorescence commitment and architecture in Arabidopsis. Science 275:80–83

Casal JJ, Sanchez RA, Deregibus VA (1986) The effect of plant density on tillering: the involvement of R/FR ratio and the proportion of radiation intercepted per plant. Environ Exp Bot 26:365–371

Chahtane H, Zhang B, Norberg M, LeMasson M, Thevenon E, Bako L et al (2018) LEAFY activity is posttranscriptionally regulated by BLADE ON PETIOLE2 and CULLIN3 in *Arabidopsis*. New Phytol 220(2):579–592. https://doi.org/10.1111/nph.15329

Cline MG (1991) Apical dominance. Bot Rev 57:318–358

Cline MG (1996) Exogenous auxin effects on lateral bud outgrowth in decapitated shoots. Ann Bot 78:255–266

Dittrich-Reed DR, Fitzpatrick BM (2013) Transgressive hybrids as hopeful monsters. Evol Biol 40:310–315

Ehrenreich IM, Stafford PA, Purugganan MD (2007) The genetic architecture of shoot branching in *Arabidopsis thaliana*: a comparative assessment of candidate gene associations vs. quantitative trait locus mapping. Genetics 176:1223–1236. https://doi.org/10.1534/genetics.107.071928

Ferguson BJ, Beveridge CA (2009) Roles for auxin, cytokinin, and strigolactone in regulating shoot branching. Plant Physiol 149:1929–1944

Foo E, Bullier E, Goussot M, Foucher F, Rameau C, Beveridge CA (2005) The branching gene RAMOSUS1 mediates interactions among two novel signals and auxin in pea. Plant Cell 17(2):464–474. https://doi.org/10.1105/tpc.104.026716

Gong X, Flores-Vergara MA, Hong JH, Chu H, Lim J, Franks RG, Liu Z, Xu J (2016) SEUSS integrates gibberellin signaling with transcriptional inputs from the SHR-SCR-SCL3 module to regulate middle cortex formation in the Arabidopsis root. Plant Physiol 170(3):1675–1683. https://doi.org/10.1104/pp.15.01501

Grbić V, Bleecker AB (2000) Axillary meristem development in *Arabidopsis thaliana*. Plant J 21(2):215–223. https://doi.org/10.1046/j.1365-313x.2000.00670.x

Greb T, Clarenz O, Schafer E, Muller D, Herrero R et al (2003) Molecular analysis of the LATERAL SUPPRESSOR gene in Arabidopsis reveals a conserved control mechanism for axillary meristem formation. Genes Dev 17:1175–1187

Haberer G, Kieber JJ (2001) Cytokinins: new insights into a classic phytohormone. Plant Physiol 128:354–362

Hansen LN, Earle ED (1997) Somatic hybrids between *Brassica oleracea* and *Sinapis alba* L. with resistance to *Alternaria brassicae*. (Berk) Sacc Theor Appl Genet 94:1078–1085

Hempel FD, Feldman LJ (1994) Bidirectional inflorescence development in *Arabidopsis thaliana*: Acropetal initiation of flowers and basipetal iniation of paraclades. Planta 192:276–286

Higuchi M, Pischke MS, Mahönen AP, Miyawaki K, Hashimoto Y, Seki M, Kobayashi M, Shinozaki K, Kato T, Tabata S et al (2004)

In planta functions of the Arabidopsis cytokinin receptor family. Proc Natl Acad Sci USA 101:8821–8826

Huai J, Zhang X, Li J, Ma T, Zha P, Jing Y, Lin R (2018) SEUSS and PIF4 coordinately regulate light and temperature signaling pathways to control plant growth. Mol Plant 11(7):928–942. https://doi.org/10.1016/j.molp.2018.04.005

Inoue T, Higuchi M, Hashimoto Y, Seki M, Kobayashi M, Kato T, Tabata S, Shinozaki K, Kakimoto T (2001) Identification of CRE1 as a cytokinin receptor from *Arabidopsis*. Nature 409:1060–1063

Jia T, Zhang K, Li F, Huang Y, Fan M, Huang T (2020) The AtMYB2 inhibits the formation of axillary meristem in Arabidopsis by repressing RAX1 gene under environmental stresses. Plant Cell Rep 39(12):1755–1765. https://doi.org/10.1007/s00299-020-02602-3

Keller T, Abbott J, Moritz T, Doerner P (2006) *Arabidopsis* REGULATOR OF AXILLARY MERISTEMS1 controls a leaf axil stem cell niche and modulates vegetative development. Plant Cell 18:598–611

Kirti PB, Narasimhulu SB, Prakash S et al (1992a) Somatic hybridization between *Brassica juncea* and *Moricandia arvensis* by protoplast fusion. Plant Cell Rep 11:318–321. https://doi.org/10.1007/BF00235090

Kirti PB, Narasimhulu SB, Prakash S, Chopra VL (1992b) Production and characterization of intergeneric somatic hybrids of *Trachystoma Ballii* and *Brassica juncea*. Plant Cell Rep 11(2):90–92. https://doi.org/10.1007/BF00235260

Kirti PB, Mohapatra T, Khanna H, Prakash S, Chopra VL (1995) *Diplotaxis catholica* + *Brassica juncea* somatic hybrids: molecular and cytogenetic characterization. Plant Cell Rep 14(9):593–597. https://doi.org/10.1007/BF00231945

Krizek BA, Blakley IC, Ho YY, Freese N, Loraine AE (2020) The *Arabidopsis* transcription factor AINTEGUMENTA orchestrates patterning genes and auxin signaling in the establishment of floral growth and form. Plant J 103(2):752–768. https://doi.org/10.1111/tpj.14769

Kumari P, Bhat SR (2019) Allohexaploid (H2) (IC0626000 INGR18031) an Indian mustard (*Brassica juncea*) germplasm with heat tolerance and resistant to *Alternaria brassicae*. Indian J Plant Genetic Resour 32(3):439

Kumari P, Bhat SR (2021) Allohexaploid (H1) (IC0628060; INGR19102), an allohexaploid (*Brassica juncea* + *Sinapis alba*) germplasm resistant to *Alternaria brassicae*, *Sclerotinia sclerotiorum* and tolerant to temperature. Indian J Plant Genet Resour 34(1):160–161

Kumari P, Singh KP (2019) Characterization of stable somatic hybrids of *Sinapis alba* and *Brassica juncea* for *Alternaria* blight, *Sclerotinia sclerotiorum* resistance and heat tolerance. Indian Res J Ext Edu 19(23):99–103

Kumari P, Singh KP, Rathore RKS (2011) Morphometric study for varietal identification of oleiferous brassicas. Proc Nat Acad Sci India Sec-B Pt IV 81:411–415

Kumari P, Bisht DS, Bhat SR (2018) Stable fertile somatic hybrids between *Sinapis alba* and *Brassica juncea* showing resistance to *Alternaria brassicae* and heat stress. Plant Cell Tissue Organ Cult 133(1):77–86. https://doi.org/10.1007/s11240-017-1362-9

Kumari P, Singh KP, Rai PK (2020a) Draft genome of multiple resistance Donor Plant *Sinapis alba*: an insight into SSRs, annotations and Phylogenetics. PLOSONE 15(4):e0231002. https://doi.org/10.1371/journal.pone.0231002

Kumari P, Singh KP, Bisht D, Kumar S (2020b) Somatic hybrids of *Sinapis alba* + *Brassica juncea*: study of backcross progenies for morphological variations, chromosome constitution and reaction to *Alternaria brassicae*. Euphytica 216:93. https://doi.org/10.1007/s10681-020-02629-3

Kumari P, Singh KP, Kumar S, Yadava DK (2020c) Development of a yellow-seeded stable allohexaploid brassica through intergeneric somatic hybridization with a high degree of fertility and resistance to *Sclerotinia Sclerotiorum*. Front Plant Sci 11:575591. https://doi.org/10.3389/fpls.2020.575591

Kumari P, Singh KP, Yadava DK (2022) Introgression of genes responsible for climate resilience in Indian mustard from allied member (*Sinapis alba* L.) through somatic hybridization, 43rd annual meeting of Plant Tissue Culture organization held on 28–30, April in NASC compelex, New Delhi

Kumari P, Singh KP, Rai PK (2023) Identification of new resistance source for Sclerotinia stem rot in backcross population of *B. juncea* + *S. Alba* allohexaploids: key to manage disease through host resistance. Euphytica 219:76. https://doi.org/10.1007/s10681-023-03208-y

Kumari P, Singh KP, Rai PK (2024a) Deciphering the genetic architecture of plant height and main shoot length in backcross introgression lines of *Sinapis alba* + *Brassica juncea* allohexaploids. Euphytica 220:3. https://doi.org/10.1007/s10681-023-03271-5

Kumari P, Singh KP, Rai PK (2024b) Mapping QTLs and candidate genes introgressed from *Sinapis alba* for siliquae related traits in second backcross progeny of allohexaploid Brassica. Euphytica 220(3):45. https://doi.org/10.1007/s10681-024-03307-4

Leyser HM, Lincoln CA, Timpte C, Lammer D, Turner J et al (1993) Arabidopsis auxin-resistance gene AXR1 encodes a protein related to ubiquitin-activating enzyme E1. Nature 364:161–164

Li AM, Wei CX, Jiang JJ, Zhang YT, Snowdon RJ, Wang Y (2009) Phenotypic variation in the progenies of somatic hybrids between Brassica napus and *Sinapis alba*. Euphytica 170:289–296

Lincoln C, Britton JH, Estelle M (1990) Growth and development of the axr1 mutants of *Arabidopsis*. Plant Cell 2:1071–1080

Long JA, Moan EI, Medford JI, Barton MK (1996) A member of the KNOTTED class of homeodomain proteins encoded by the STM gene of Arabidopsis. Nature 379:66–69

Lynn K, Fernandez A, Aida M, Sedbrook J, Tasaka M, Masson P, Barton MK (1999) The PINHEAD/ZWILLE gene acts pleiotropically in Arabidopsis development and has overlapping functions with the ARGONAUTE1 gene. Development 126:469–481

Lysak MA, Koch MA, Pecinka A, Schubert I (2005) Chromosome triplication found across the tribe. Brassiceae Genome Res 15(4):516–525. https://doi.org/10.1101/gr.3531105

Mallet J (2007) Hybrid speciation. Nature 446:279–283

McConnell JR, Barton MK (1995) Effect of mutations in the PINHEAD gene of Arabidopsis on the formation of shoot apical meristem. Dev Genet 16:358–366

McSteen P, Leyser O (2005) Shoot branching. Annu Rev Plant Biol 56:353–374

Meng L, Li H, Zhang L, Wang J (2015) QTL IciMapping: Integrated software for genetic linkage map construction and quantitative trait locus mapping in biparental populations. Crop J 3(3):269–283. https://doi.org/10.1016/j.cj.2015.01.001

Moussian B, Schoof H, Haecker A, Jurgens G, Laux T (2006) Role of the ZWILLE gene in the regulation of central shoot meristem cell fate during *Arabidopsis* embryogenesis. EMBO J 17:1799–1809

Muller D, Schmitz G, Theres K (2006) Blind homologous R2R3 myb genes control the pattern of lateral meristem initiation in *Arabidopsis*. Plant Cell 18:586–597

Nambeesan SU, Mandel JR, Bowers JE et al (2015) Association mapping in sunflower (*Helianthus annuus* L.) reveals independent control of apical vs. basal branching. BMC Plant Biol 15:84. https://doi.org/10.1186/s12870-015-0458-9

Napoli CA, Ruehle J (1996) New mutations affecting meristem growth and potential in Petunia hybrida Vilm. J Hered 87:371–377

Nelson MN, Lydiate DJ (2006) New evidence from *Sinapis alba* L. for ancestral triplication in a crucifer genome. Genome 49:230–238. https://doi.org/10.1139/G05-099

Nishimura C, Ohashi Y, Sato S, Kato T, Tabata S, Ueguchi C (2004) Histidine kinase homologs that act as cytokinin receptors possess

overlapping functions in the regulation of shoot and root growth in Arabidopsis. Plant Cell 16:1365–1377
Ongaro V, Leyser O (2008) Hormonal control of shoot branching. J Exp Bot 59:67–74
Ouellet F, Overvoorde PJ, Theologis A (2001) IAA17/AXR3: biochemical insight into an auxin mutant phenotype. Plant Cell 13(4):829–841. https://doi.org/10.1105/tpc.13.4.829
Rameau C, Bertheloot J, Leduc N, Andrieu B, Foucher F, Sakr S (2015) Multiple pathways regulate shoot branching. Front Plant Sci 5:741. https://doi.org/10.3389/fpls.2014.00741
Reinhardt D, Kuhlemeier C (2002) Plant architecture. EMBO Rep 3:846–851
Sarlikioti V, de Visser PHB, Buck-Sorlin GH, Marcelis LFM (2011) How plant architecture affects light absorption and photosynthesis in tomato: toward anideotype for plant architecture using a functional–structural plant model. Ann Bot 108:1065–1073
Shimizu-Sato S, Mori H (2001) Control of outgrowth and dormancy in axillary buds. Plant Physiol 127:1405–1413
Shimizu-Sato S, Tanaka M, Mori H (2009) Auxin-cytokinin interactions in the control of shoot branching. Plant Mol Biol 69:429–435
Singh RK, Chaudhary BD (1977) Biometrical methods in quantitative genetic analysis. Kalyani, New Delhi, p 304
Singh KP, Kumari P, Rai PK (2021a) Current status of the disease-resistant gene(s)/QTLs, and strategies for improvement in *Brassica juncea*. Front Plant Sci 12:617405. https://doi.org/10.3389/fpls.2021.617405
Singh KP, Kumari P, Yadava DK (2021b) Introgression and QTL mapping conferring resistance for *Alternaria brassicae* in the backcross progeny of *Sinapis alba* + *Brassica juncea* somatic hybrids. Plant Cell Rep 40:2409–2419. https://doi.org/10.1007/s00299-021-02785-3
Singh KP, Kumari P, Yadava DK (2022a) Development of Denovo transcriptome assembly and SSRs in Allohexaploid Brassica with functional annotations and identification of heat-shock proteins for thermotolerance. Front Genet 13:958217. https://doi.org/10.3389/fgene.2022.958217
Singh KP, Kumari P, Raipuria RK, Rai PK (2022b) Development of genome-specific SSR markers for the identification of introgressed segments of *Sinapis alba* carrying genes for blight resistance in the *Brassica juncea* background. 3Biotech 12:332. https://doi.org/10.1007/s13205-022-03402-0
Singh KP, Kumari P, Rai PK (2023) Phenotypic characterization and resistance response to *Sclerotinia sclerotiorum* of backcross lines developed from stable allohexaploids of *Sinapis alba* + *Brassica juncea*. Euphytica 219:34. https://doi.org/10.1007/s10681-023-03160-x
Soltis PS, Soltis DE (2009) The role of hybridization in plant speciation. Annu Rev Plant Biol 60:561–588
Sorefan K, Booker J, Haurogne K, Goussot M, Bainbridge K et al (2003) MAX4 and RMS1 are orthologous dioxygenase-like genes that regulate shoot branching in *Arabidopsis* and pea. Genes Dev 17:1469–1474
Stirnberg P, Chatfield SP, Leyser HM (1999) AXR1 acts after lateral bud formation to inhibit lateral bud growth in *Arabidopsis*. Plant Physiol 121:839–847
Stirnberg P, van De Sande K, Leyser HM (2002) MAX1 and MAX2 control shoot lateral branching in *Arabidopsis*. Development 129:1131–1141
Talbert PB, Adler HT, Parks DW, Comai L (1995) The REVOLUTA gene is necessary for apical meristem development and for limiting cell divisions in the leaves and stems of *Arabidopsis thaliana*. Development 121:2723–2735
Ungerer MC, Halldorsdottir SS, Modliszewski JL, Mackay TF, Purugganan MD (2002) Quantitative trait loci for inflorescence development in *Arabidopsis thaliana*. Genetics 160:1133–1151
Ungerer MC, Halldorsdottir SS, Purugganan MD, Mackay TF (2003) Genotype-environment interactions at quantitative trait loci affecting inflorescence development in *Arabidopsis thaliana*. Genetics 165:353–365
Wang J, Gao Y, Kong Y, Jiang J, Li A, Zhang Y, Wang Y (2014) Abortive process of a novel rapeseed cytoplasmic male sterility line derived from somatic hybrids between *Brassica napus* and *Sinapis alba*. J Integr Agric 13(4):741–748. https://doi.org/10.1016/S2095-3119(13)60584-5
Wang YP, Sonntag K, Rudloff E, Chen JM (2005) Intergeneric somatic hybridization between *Brassica napus* L. and *Sinapis alba* L. J Integr Plant Biol 47(1):84–91. https://doi.org/10.1111/j.1744-7909.2005.00009.x
Ward SP, Leyser O (2004) Shoot branching. Curr Opin Plant Biol 7:73–78
Weigel D, Alvarez J, Smyth DR, Yanofsky MF, Meyerowitz EM (1992) LEAFY controls floral meristem identity in *Arabidopsis*. Cell 69:843–859
Yaish MWF, Guevara DR, El-Kereamy A, Rothstein SJ (2010) Axillary shoot branching in plants. In: Pua EC, Davey MR (eds) Plant developmental biology–biotechnological perspectives. Springer, Berlin, pp 37–52
Zhu H, Hu F, Wang R, Zhou X, Sze SH, Liou LW, Barefoot A, Dickman M, Zhang X (2011) *Arabidopsis* Argonaute10 specifically sequesters miR166/165 to regulate shoot apical meristem development. Cell 145(2):242–256. https://doi.org/10.1016/j.cell.2011.03.024

Publisher's Note Springer Nature remains neutral with regard to jurisdictional claims in published maps and institutional affiliations.

Springer Nature or its licensor (e.g. a society or other partner) holds exclusive rights to this article under a publishing agreement with the author(s) or other rightsholder(s); author self-archiving of the accepted manuscript version of this article is solely governed by the terms of such publishing agreement and applicable law.